Assimilation of Pseudo-Tree-Ring-Width observations into an Atmospheric General Circulation Model

Walter Acevedo[1,2], Bijan Fallah[1], Sebastian Reich[2], and Ulrich Cubasch[1]

[1]Institut für Meteorologie, Freie Universität Berlin, Carl-Heinrich-Becker-Weg 6-10, 12165 Berlin, Germany.
[2]Institut für Mathematik, Universität Potsdam, Karl-Liebknecht-Strasse 24-25, 14476 Potsdam, Germany.

Correspondence to: Bijan Fallah (info@bijan-fallah.com)

Abstract. Paleoclimate Data Assimilation (DA) is a promising technique to systematically combine the information from the climate model simulations and the proxy records. Here we investigate the assimilation of Tree-Ring-Width (TRW) chronologies into an atmospheric global climate model using Ensemble Kalman Filter (EnKF) techniques and a process-based tree-growth forward model as observation operator. Our results, within a perfect-model experiment setting, indicate that the "on-line DA"
5   approach did not outperform the "off-line" one, despite its considerable additional implementation complexity. On the other hand, it was observed that the nonlinear response of tree-growth to surface temperature and soil moisture does deteriorate the operation of the time-averaged EnKF methodology. Moreover, for the first time we show that this skill loss appears significantly sensitive to the structure of growth rate function, used to represent the Principle of Limiting Factor (PLF)s within the forward model. Additionally, our experiments showed that the error reduction achieved by assimilating a pseudo-TRW chronologies
10   is modulated by the strength of the yearly internal variability of the model. This result might help the dendrochronology community to optimize their sampling efforts.

1   Introduction

The low-frequency temporal variability of the climate system can not be estimated from the available time span of instrumental climate records. Accordingly, paleoclimate reconstruction must necessarily rely on the usage of the paleoclimate proxy records.
15   These natural archives exhibit several problematic features, e.g., low time-resolution, sparse and irregular spatial distribution, complex nonlinear response to climate and high noise levels. Therefore the proper extraction of the climate signal therein contained can often remain opaque (Evans et al., 2013). At present, many different paleoclimate modeling ideas have been proposed, e.g., data-driven statistical techniques, climate model hindcasts, and Bayesian probabilistic methods (see Crucifix (2012) as a recent review). Among this plethora of approaches, DA methodologies are today particularly appealing as they
20   allow to systematically combine the information of paleoclimate records with the dynamical consistence of climate simulations (Brönnimann, 2011; Hakim et al., 2016). So far, several very diverse paleo-DA schemes have been investigated, including (i) pattern nudging (von Storch et al., 2000), forcing singular vectors (Barkmeijer et al., 2003; van der Schrier and Barkmeijer, 2005), 4D-Var (Paul and Schäfer-Neth, 2005; Kurahashi-Nakamura et al., 2014), particle filters (Annan and Hargreaves, 2012; Dubinkina et al., 2011; Dubinkina and Goosse, 2013; Mathiot et al., 2013; Matsikaris et al., 2015) and EnKF (Huntley and

Hakim, 2010; Bhend et al., 2012; Pendergrass et al., 2012; Steiger et al., 2014) (see (Hughes and Ammann, 2009; Widmann et al., 2010; Hakim et al., 2013) as reference).

An important difference between paleo-DA and traditional meteorological DA, is that the assimilation period might be very long compared to the time scales of the dynamical model. Under these conditions, the randomizing action of chaotic model dynamics becomes dominant and consequently the forecast appears completely decorrelated from the previous analysis state. This phenomenon, currently referred to as "off-line regime", has been observed in several paleo-DA studies (Huntley and Hakim, 2010; Bhend et al., 2012; Pendergrass et al., 2012; Matsikaris et al., 2015). Furthermore, some recent studies have assumed from the beginning the off-line condition and removed the reinitialization step after assimilation, giving raise to "off-line DA techniques" (Steiger et al., 2014; Dee et al., 2016; Hakim et al., 2016).

A typical assumption in most of the paleo-DA studies so far conducted is that the climate-proxy relation is linear. Nonetheless, currently it is widely recognized that climate proxies are the result of complex recording processes, which can have physical, chemical and biological nature. The dendrochronologists usually investigate the climate impact on tree-ring growth by empirical–statistical methods (Vaganov et al., 2006). More realistic methodologies have been recently sculpted by the paleoclimate community to investigate the climate-proxy relation that consider the distinct processes whereby the climate signal is recorded in proxy archives. Proxy forward modeling (Hughes et al., 2010; Evans et al., 2013) appears to be one of the most promising methodologies in this area. In a proxy forward model the climate forcing is used as input data for producing the artificial proxy records which can be directly compared with the actual ones. One application of proxy forward models is to predict the evolution of proxy archives (Vaganov et al., 2006). They can also be applied as climate reconstruction strategies by using the probabilistic inversion methods like Bayesian hierarchical modeling (Tolwinski-Ward, 2012), Markov Chain Monte Carlo (MCMC) (Boucher et al., 2014) and DA (Hughes et al., 2010).

Several recent studies have investigated the applicability of process-based forward models into a paleo-DA setting, in the realism of DA-based climate reconstructions (Hughes et al., 2010; Acevedo et al., 2015; Dee et al., 2016; Hakim et al., 2016). Acevedo et al. (2015) [AC15, hereafter] utilized the process-based TRW forward model Vaganov-Shashkin-Lite (VSL) (Tolwinski-Ward et al., 2011) and an online EnKF scheme, to assimilate TRW records into a chaotic 2-scale dynamical system as a toy model. They found that the non-linearities of the forward model may deteriorate the performance of the EnKF. Furthermore, they observed that this loss of skill may be ameliorated by means of a Fuzzy Logic (FL)-based extension of VSL model. Matsikaris et al. (2015) compared an off-line and an on-line ensemble-based DA ("degenerat particle filter") and showed that the both methods outperform the model without DA. They concluded that in the off-line method temporal consistency of the model is lost. However, they encouraged to use a full particle filter strategy instead of a degenerate one. On the other hand, Dee et al. (2016) used three different nonlinear proxy forward models (including VSL) and an off-line EnKF scheme to assimilate TRW, coral and ice core records into two different isotope-enabled Atmospheric General Circulation Model (AGCM). They demonstrated that the linear-univariate models for tree ring width may not capture the AGCM's climate, especially for regions where the tree's growth is dominated by moisture.

This paper follows the rationale of AC15, but within a more realistic scenario, where an AGCM is used as dynamical system and the observational network resembles the currently available TRW chronologies. The purpose of this study is then

to contribute to the present knowledge of paleo-DA techniques by addressing the following two questions: (i) Does the off-line regime naturally appear for the assimilation of TRW records into a AGCM? and (ii) is the Fuzzy Logic (FL)-based extension of VSL model still useful to improve the performance of EnKF when a climate model is used?

This study is structured as follows: in section 2 we describe the DA technique, the TRW forward model and the climate
5   model as well as the experimental setting used. Our numerical results are shown in section 3, followed by a discussion in section 4.

2   Materials and Methods

2.1   Data Assimilation Basics

The term DA designates in this paper the process of estimating the state of a system using observations and the physical
10   laws governing the evolution of the system as represented in a numerical model (Talagrand, 1997). In a typical DA scheme, a dynamical model is integrated in time until observations become available. Afterwards, the predicted state, also known as forecast, is "updated" using the observational information in order to obtain a corrected state, also known as the analysis. Finally, the model is reinitialized from the analysis state and propagated in time until the next assimilation time, completing the so-called "analysis" cycle. DA methods have evolved from very empirical approaches, such as Newtonian relaxation,
15   to probabilistic ones that attempt to estimate the Probability Density Function (PDF) of the model state conditional to the observations (see Kalnay (2003); Lahoz et al. (2010); Reich and Cotter (2015) as reference materials).

Among the currently available DA techniques, EnKF (Burgers et al., 1998) occupies an outstanding position due to several reasons. It offers an appealing trade-off between accuracy and computational expenses. It works robustly for sparse observation networks and moderate number of ensemble members (Whitaker et al., 2009). Furthermore, EnKF's implementation does not
20   require any modification of the model's code and uncertainty estimates can be directly obtained from the ensemble spread (Hamill, 2006). The main disadvantage of EnKF, within a paleoclimate setting, is its inability to handle non-Gaussian PDFs, which can easily arise from the nonlinearities of climate models and observation operators. Recently, there have been several developments in the field of non-linear DA for high-dimensional systems (Van Leeuwen et al., 2015), however at the present fully non-Gaussian DA techniques are still prohibitively expensive to run for general circulation climate models.

25 2.1.1   Kalman Filter

Within the Kalman Filter (KF) (Kalman, 1960), the PDF of forecast state $p(\mathbf{x})$ is assumed to be given by a Gaussian function with mean $\mathbf{x}^f$ and covariance $\mathbf{P}^f$:

$$p(\mathbf{x}) \propto \exp(-\frac{1}{2}(\mathbf{x} - \mathbf{x}^f)^T (\mathbf{P}^f)^{-1} (\mathbf{x} - \mathbf{x}^f)). \tag{1}$$

The observations $\mathbf{y}(t_j)$ are also assumed to have Gaussian errors and therefore the conditional probability of the observation vector $\mathbf{y}$ given the state $\mathbf{x}$ is:

$$p(\mathbf{y} \mid \mathbf{x}) \propto \exp(-\frac{1}{2}(\mathbf{y} - \widehat{\mathrm{H}}\mathbf{x}^f)^T \mathbf{R}^{-1}(\mathbf{y} - \widehat{\mathrm{H}}\mathbf{x}^f)), \tag{2}$$

where $\widehat{\mathrm{H}}$ is the observation operator and $\mathbf{R}$ is the observation covariance matrix, respectively. Following the Bayes theorem, the conditional probability of the state given the observations, i.e., the analysis PDF, is:

$$p(\mathbf{x} \mid \mathbf{y}) \propto \exp(-\frac{1}{2}(\mathbf{x} - \mathbf{x}^f)^T (\mathbf{P}^f)^{-1}(\mathbf{x} - \mathbf{x}^f) - \frac{1}{2}(\mathbf{y} - \widehat{\mathrm{H}}\mathbf{x}^f)^T \mathbf{R}^{-1}(\mathbf{y} - \widehat{\mathrm{H}}\mathbf{x}^f)). \tag{3}$$

Finally, assuming that $\widehat{\mathrm{H}}$ is a linear function, $p(\mathbf{x} \mid \mathbf{y})$ is also a Gaussian function whose mean and covariance can be calculated by the so-called Kalman update equations (Lorenc, 1986):

$$\mathbf{x}^a = \mathbf{x}^f + \mathbf{K}(\mathbf{y} - \widehat{\mathrm{H}}\mathbf{x}^f), \tag{4}$$

$$\mathbf{P}^a = (\mathbf{I} - \mathbf{K}\widehat{\mathrm{H}})\mathbf{P}^f; \tag{5}$$

where the Kalman gain matrix $\mathbf{K}$ is given by:

$$\mathbf{K} = \mathbf{P}^f \widehat{\mathrm{H}}^\dagger (\widehat{\mathrm{H}}\mathbf{P}^f \widehat{\mathrm{H}}^\dagger + \mathbf{R})^{-1}. \tag{6}$$

2.1.2 Ensemble Kalman Filter (EnKF)

For realistic geophysical models, the dimensionality of the model state can be very high and then the calculation and storage of the covariance matrices can be prohibitively expensive. A solution to this problem is provided by the EnKF (Evensen, 1994), which uses an ensemble of model states ($\mathbf{X}(t) = (\mathbf{x}_1, \ldots, \mathbf{x}_m)$) to approximate KF equations. Following this approach, the mean and covariance of the forecast take the following form:

$$\langle \mathbf{X}_f \rangle = \frac{1}{m}\sum_{i=1}^{m} \mathbf{x}_i^f, \ \ \mathbf{P}^f = \frac{1}{m-1}\mathbf{X}_f{}'(\mathbf{X}_f{}')^T. \tag{7}$$

Here $\mathbf{X}_f{}' \in \mathbb{R}^{n \times m}$ denotes the forecast ensemble deviation matrix:

$$\mathbf{X}_f{}' = \mathbf{X}_f - \langle \mathbf{X}_f \rangle \mathbf{e}^T. \tag{8}$$

where $\mathbf{e} = (1, \ldots, 1) \in \mathbb{R}^m$. An analysis ensemble whose covariance satisfies equation 5 can be generated in different ways, which can be classified into two main families: stochastic and deterministic filters (Hamill, 2006). In the stochastic approach an observational ensemble $\mathbf{Y}$ is generated by adding realizations of the observational noise to the observation vector $\mathbf{y}$. The analysis ensemble is then created by the following updating equation:

$$\mathbf{X}_a = \mathbf{X}_f + \mathbf{K}\left(\mathbf{Y} - \widehat{\mathrm{H}}\mathbf{X}_f\right). \tag{9}$$

In the deterministic approach, instead of creating an ensemble of observations, the analysis mean and deviations are calculated using update formulae which do not involve random numbers (see Tippett et al. (2003) as reference).

A practical problem of EnKF schemes, is that due to the limited ensemble size, the forecast uncertainty is usually under-estimated. This leads to an excessive confidence on the forecast and after several assimilation cycles the observations may be completely ignored. This situation is normally avoided by means of an *ad hoc* procedure known as "covariance inflation", where the forecast covariance matrix is multiplied by a constant greater than one. For the experiments presented in this paper, we employed ensembles of 24 members and constant multiplicative inflation of 1% after the ensemble update. Another unde-sired consequence of the limited ensemble size, is that the ensemble state at any gridpoint will present non-negligible spurious correlations with observations located far apart in space. This difficulty is solved using another *ad hoc* procedure known as "covariance localization". Here we utilize the so-called R-localization (Hunt et al., 2007), where the elements of the observa-tion error covariance matrix are multiplied by a function that increases exponentially with distance. This is achieved using the following formula:

$$R_{loc} = R * \exp\left((r_h/2\lambda_h)^2 + (r_v/2\lambda_v)^2\right) \tag{10}$$

where r_h and r_v stand for the horizontal and vertical distances, respectively. Their corresponding scaling parameters were set to the values $\lambda_h = 500$ Km and $\lambda_v = 0.4 \ln p$.

2.1.3 Time-Averaged Ensemble Kalman Filter (EnKF)

The EnKF algorithm was initially designed to estimate the instantaneous state of a model given instantaneous observations. As a consequence, EnKF cannot be directly applied to paleoclimate data given that the observational information present in proxy records is typically the average of a function of the state over long time periods. A solution to this conflict is provided by the time-averaged Ensemble Kalman Filter (EnKF) (Dirren and Hakim, 2005), where the instantaneous forecast is decomposed into its time-averaged part and the anomalies around it. Afterwards, the original EnKF update formula is used to assimilate the time-averaged observations into the time-averaged forecast, obtaining the time-averaged analysis. Finally, the instantaneous analysis is form by adding the unaltered time-averaged forecast anomalies to the time-averaged analysis. This approach is based on the assumption that the observations can only contain time-averaged information (Dirren and Hakim, 2005).

An crucial aspect of time-averaged DA is the off-line regime, which manifest itself as a complete lack of estimation skill for the forecast quantities. This behavior was first observed for the time-averaged Ensemble Kalman Filter (EnKF) applied to a quasi-geostrophic atmospheric jet model (Huntley and Hakim, 2010; Pendergrass et al., 2012). Afterwards, several studies have used the simplified off-line time-averaged Ensemble Kalman Filter (EnKF) approach with global climate models (Bhend et al., 2012; Steiger et al., 2014; Dee et al., 2016) assuming the presence of the off-line regime. However, to our knowledge, there had not been numerical evidence of the onset of off-line conditions for a full time-averaged Ensemble Kalman Filter (EnKF) algorithm applied to a AGCM. As mentioned in the introduction, filling this knowledge gap is one the objectives of this paper.

2.2 TRW Forward Model

The Vaganov-Shashkin-Lite (VSL) model for TRW chronologies offers an intermediate complexity approach between ecophys-iological and completely data-driven models (Tolwinski-Ward et al., 2011; Tolwinski-Ward, 2012), where the climate-driven

component of tree-ring growth is parametrized by way of a simple representation of the Principle of Limiting Factor (PLF) (Fritts, 1976). The biological concept of PLF states that the pace at which a plant develops is controlled by the single basic growth resource, typically either energy or water, that is in shortest supply. Within VSL the limiting factors considered are near-surface air temperature (T) and soil moisture (M). These variables influence tree growth by means of "growth response"

5   functions g_T and g_M using a piece-wise linear "standard ramp" function (Tolwinski-Ward et al., 2014):

$$\Psi(u) = \begin{cases} 0 & \text{if} \quad 0 \geqslant u \\ u & \text{if} \quad 0 < u \leqslant 1 \\ 1 & \text{if} \qquad u > 1, \end{cases}$$

VSL's growth responses at a particular time is expressed as:

$$g_T = \Psi\left(\frac{T - T^L}{T^U - T^L}\right) \tag{11}$$

and

10   $$g_M = \Psi\left(\frac{M - M^L}{M^U - M^L}\right). \tag{12}$$

Where T^L and M^L denote minimum thresholds for temperature and moisture below which there is no growth, and T^U and M^U are upper thresholds above which tree growth is optimal. Afterwards, the growth rate G_{MIN} is determined by the smallest growth response, i.e.,

$$G_{MIN} = \min\{g_T, g_M\}, \tag{13}$$

15   The yearly TRW values W are obtained as following:

$$W_n = \int_{t_n - \tau}^{t_n} G_{MIN}(t) I(t) \, dt. \tag{14}$$

Where I is the relative local insolation.

2.2.1 VSL from the Fuzzy Logic Viewpoint

The term Fuzzy Logic (FL) was coined by Zadeh (1975) and refers to a mathematical theory which has been very successful at

20   modeling complex systems involving imprecise data and vague knowledge of the underlying mechanisms. Since its introduction, FL has greatly influenced many disciplines, most notably control theory (Nguyen et al., 2002). Within the environmental sciences, FL has been applied in ecological and hydrological modeling (Marchini, 2011; Salski, 2006; Se, 2009). Regarding climate proxy forward modeling, AC15 recently showed that VSL model can be completely embedded into the framework of FL. Within this reinterpretation, the growth response function g_T (g_M) corresponds to the membership function to the set

S_T (S_M) of optimal temperature (moisture) conditions for tree growth. Temperature (moisture) values lying below T^L (M_L) present null values for g_T (g_M) and accordingly do not belong to S_T (S_M). On the other hand, temperature (moisture) values lying above T^U (M_U) lead to g_T (g_M) values equal to 1, meaning they belong completely to S_T (S_M). All the other temperature (moisture) conditions present growth responses between 0 and 1 and consequently they are considered to belong partially
5   to S_T (S_M). This idea of partial membership is the basis of fuzzy logic and the sets defined this way are called fuzzy sets. Furthermore, the intersection of the fuzzy sets S_T and S_M is again a fuzzy set $S_{T \wedge M}$, whose membership function can be calculated by evaluating the minimum between G_T and G_M:

$$g_{T \wedge M} = \min\{g_T, g_M\} \tag{15}$$

Equation 15 is completely equivalent to the equation 14. Then VSL's growth rate function can be interpreted as the mem-
10   bership function for the fuzzy intersection set $S_{T \wedge M}$. In FL theory, the minimum function (Eq. 15) is one of the most popular representations of the intersection operation, however it is not the only, existing actually a whole family of appropriate functions referred to as t-norms (see Nguyen et al. (2002)). In AC15 a number of t-norms was tested as replacement for VSL's growth rate function within a highly simplified paleo-DA setting. In particular it was found that the product t-norm $g_{T \wedge M} = g_T \cdot g_M$ might improve significantly the performance of the time-averaged EnKF technique. Accordingly, beside the minimum t-norm
15   we consider also in this paper the product growth response VSL with Product t-norm (VSL-Prod):

$$G_{PROD} = g_T \cdot g_M. \tag{16}$$

2.3 Experimental Design

Following the rationale used in the experiments of AC15, a set of "perfect model" Observation System Simulation Experiments (OSSE)s (see fig. 1) was conducted using SPEEDY model (Molteni, 2003) as dynamical system and VSL forward model as
20   observation operator. The time-averaged state of the atmosphere is estimated via the EnKF approach of Dirren and Hakim (2005). In the following, we describe in detail each of the components of our experimental setting.

2.3.1 Atmospheric General Circulation Model

The Simplified Parametrizations, primitivE-Equation Dynamics (SPEEDY) model (Molteni, 2003) is an intermediate complexity AGCM comprising a spectral dynamical core and a set of simplified physical parametrizations, based on the same principles
25   as state-of-the-art AGCM but tailored to work with just a few vertical levels. Regarding the ocean, SPEEDY offers two possible configurations: (i) *PRESCRIBED* where the sea surface temperature is directly imposed as forcing and (ii) *SLAB* where the model is coupled to a slab ocean model ("q-flux adjusted mixed layer model") forced by climatological ocean dynamics. Despite of its low resolution and the relative low complexity of its parameterizations, SPEEDY still captures many observed global climate features in a realistic way, while its computational cost is at least one order of magnitude lower than the one of
30   sophisticated state-of-the-art AGCM's at the same horizontal resolution (Molteni, 2003). The latter makes SPEEDY specially suitable for studies involving long ensemble runs, like the ones necessary for this study.

The SPEEDY model was embedded by Miyoshi (2005) into the so called SPEEDY-Local Ensemble Transform Kalman Filter (LETKF) framework, which offers a parallel implementation of LETKF (Hunt et al., 2007). Among the different flavors of EnKF, LETKF is particularly promising for high resolution models given that the calculation of the analysis for a particular grid point requires only the information of the neighboring grid points. Therefore, LETKF offers outstanding scalability properties.
SPEEDY-LETKF is an open-source software which have already been widely used for several DA studies (Li et al., 2009; Miyoshi, 2010; Lien et al., 2013; Ruiz et al., 2013; Amezcua et al., 2014). Here, SPEEDY-LETKF was extended to allow the assimilation of time averaged linear observations and pseudo-TRW observations.

2.3.2 Perfect Model Experiments

Given a dynamical climate model and a DA scheme, forecast and analysis errors arise from many different sources, e.g. model imperfections, inadequacy of the DA strategy and insufficiency of observational information, all which interact with each other in practice. In order to disentangle the effects of these error sources, a DA scheme is typically tested under simplified conditions by means of perfect numerical experiments, currently known as OSSE, whose realism level is gradually increased. An OSSE consists of (i) a single model trajectory $\mathbf{x}^{\text{NATURE}}$, typically referred to as "true" run or "nature" run, that is used as prediction target, (ii) pseudo-observations created by applying the observation operator to $\mathbf{x}^{\text{NATURE}}$ and adding simulated observational noise, and (iii) an observationally constrained run $\mathbf{X}^{\text{DA}}$, obtained by performing a sequence of analysis cycles where the pseudo-observations are assimilated (see Fig. 1). The nature run is normally generated by running the dynamical model starting from a random sample of the model climatology. Notice that thanks to the availability of the truth model evolution for an OSSE, the forecast and analysis skill of the observationally constrained run can be directly assessed, using for example the Root Mean Square Error (RMSE) of the ensemble mean:

$$\mathbf{RMSE}(\langle \mathbf{X}^{\text{DA}} \rangle) = \left(\overline{\left(\mathbf{x}^{\text{NATURE}} - \langle \mathbf{X}^{\text{DA}} \rangle \right)^2} \right)^{\frac{1}{2}}, \tag{17}$$

where $\overline{}$ and $\langle \ \rangle$ denote the time and ensemble mean operators, respectively. An additional run frequently performed for OSSE involving ensemble DA methods, is a free ensemble run $\mathbf{X}^{\text{FREE}}$, where no observations are assimilated and then the ensemble just freely evolve under the action of the model dynamics. $\mathbf{X}^{\text{FREE}}$ is intended to provide a benchmark of performance, against which it is possible to asses the the added value of the DA scheme.

The modified version of SPEEDY-LETKF is used to carry out a set of standard OSSEs (Fig. 1). First a simple representation of the PLF (VSL controlled only by Temperature (VSL-T)) is utilized for two sets of experiments under different ocean conditions:

• *PRESCRIBED experiment* is forced by the boundary conditions included in the version 41 of the code, which comprises the sea surface temperature (SST) anomalies from 1854 to 2010 with respect to the period 1979 to 2008 derived from NOAA_ERSST_V3 dataset (Smith et al., 2008; Xue et al., 2003), as well as climatological maps derived from input data of the European Centre for Medium-Range Weather Forecasts (ECMWF)'s reanalysis (Gibson et al., 1997). At the surface boundaries the model requires the climatological maps of sea surface temperature, sea ice fraction, surface temperature at the top of the soil, moisture in the top soil layer and the root-zone layer, snow depth, bare-surface albedo, fraction of land-surface vegetation.

At the top of the atmosphere, the model calculates the flux of incoming solar radiation from astronomical formulae (Molteni, 2003). The solar radiation absorption by ozone in the stratosphere follows empirical functions with seasonal variability. The latitudinal variability of the optical depth depends on the daily averaged zenith angle (Molteni, 2003). The climatological fields are derived for the period 1981-1990 to have a better balance for warm and cold El Niño-Southern Oscillation (ENSO) events (Molteni, 2003). This procedure follows the AMIP-type experiments (Herceg Bulić and Kucharski, 2012).

- *SLAB experiment* is coupled with a slab ocean model forced by climatological ocean dynamics and no initialization is used. The model starts from a spun up state. We consider two representations of the PLF: the "minimum" (G_{MIN}) and the "product" (G_{PROD}) t-norms. Initially, a one-year long spin-up run is performed for all experiments, starting from January 1st, 1860. The final state of this model trajectory is subsequently used as initial condition for a 150 year long nature ("true") run. The ensemble runs with and without DA are identically initialized from a set of states gathered daily from the last two months of the spin-up run (lagged 2 day initialization). Notice that the nature ("true") run and the different ensemble runs (forecasts) are generated with the same time varying forcing fields.

2.3.3 Observation Generation

Pseudo-TRW observations are produced following VSL's formulation, plus a final white noise addition step, where random draws from a Gaussian distribution are imposed on the time averaged observations. In a perfect model experiment it is usually assumed that the measurements' errors are not correlated in time (no memory) and the "white noise" is added to the observations (McShane and Wyner, 2011; Dee et al., 2016). Surface temperature data was extracted from the model, while soil moisture was taken from the surface boundary conditions. Notice that temperature is a prognostic variable of the model, whereas soil moisture is a prescribed variable with yearly periodicity. It is worthwhile to mention that although soil moisture is not a prognostic variable of SPEEDY, it does affect prognostic variables, such us humidity, through the parametrizations. We place a station at every grid box where at least one actual TRW chronology from the database of Breitenmoser et al. (2014) is present. This strategy yields a realistic observational network comprising 257 stations (see figure 2). Concerning the configuration of the observation operator, for our experiment involving SPEEDY we focus on the effect of the first VSL's nonlinearity, i.e., the shifting of recorded variable (growth is limited by either temperature or moisture). Consequently, we configure VSL so that no thresholding takes place. This is done by setting the upper and lower response thresholds to the maximum and minimum values during the nature (true) run, respectively, so that the response functions reduce to linear rescaling operators (ref. AC15).

3 Results

Given the annual resolution of TRW chronologies, we study the filter performance for yearly averaged values of near surface temperatures. We focus our analysis on temperature due to the larger error reduction in this field as compared to other variables (*eg*, humidity, u-wind, v-wind) when DA is applied. The behavior of ensemble runs is monitored by means of RMSE for the near surface temperature. The results are shown as: 1) time-series of globally averaged temperature RMSE, 2) histograms of these time-series and 3) maps of time-averaged (150 years) temperature RMSEs. We begin with the investigation of the

performance of the online and offline DA simulations. Then the performance of DA skill is tested for two different growth functions. Afterwards, we examine the performance of the off-line DA for different observational errors. Finally, the effect of using the time-varying soil moisture fields on the performance of DA approach is tested.

3.1 Free Ensemble Spread and Error

An AGCM is an example of non-autonomous system and accordingly the evolution of its state is determined by both the atmospheric dynamics and the external forcing. The influences of these two distinct factors can be disentangled to some extent by considering atmospheric variability to be a superposition of an internal component, caused by the intrinsic dynamics, and an external one, resulting from the variations of the boundary conditions (Deza et al., 2014). Under this assumption, internal and external variability can be separated by way of a free ensemble run, using the ensemble mean as an estimate of the forced component. The magnitude of the internal variability can then be estimated from the ensemble spread. Note that using an ensemble DA method is only beneficial in the presence of internal variability, given that the forced variability can be well described by an unconstrained ensemble run (free ensemble run). The time averaging operator acts as a low pass filter that reduces the amplitude of fluctuations with time scales shorter than the averaging period. Subsequently, geographical areas dominated by fast processes, compared to averaging period, tend to present constant mean values, or equivalently no internal time averaged variability. In the case of TRW chronologies, the characteristic one-year averaging period is long for atmospheric phenomena, and as consequence several areas show very low yearly internal variability for certain variables. A clear example of this is temperature around the equator (see figure 3a) where the temperature variability is dominated by the daily cycle and accordingly is strongly attenuated by the yearly averaging. On the other hand, planetary scale patterns are not completely stationary and fluctuate over longer time scales. These low-frequency processes introduce internal variability in the yearly means, as can be seen in figure 3a. Maximum temperature spread occurs near the surface at high latitudes around $\pm 70°$. These yearly internal variability maxima can be related to leading modes of variability of the global circulation, such as the "annular modes" (e.g., ENSO) (Thompson and Wallace, 2000), migrations of the Inter Tropical Convergence Zone (ITCZ) (Schneider et al., 2014), as well as displacements of the jet stream (Woollings et al., 2011).

An important consequence of the spatially heterogeneous yearly internal variability of SPEEDY is that the nature (true) run variables at geographical areas with low internal variability can be well predicted by the ensemble mean of the free ensemble run, as it can be seen in figure 3b for the tropical surface temperature. On the other hand, RMSE extremes take place in areas of maximal internal variability (compare figures 3a and 3b). Generally, the error of the free ensemble run, used as a predictor of the nature (true) run, is essentially the projection of the nature (true) run trajectory on the internal variability component (see schematic in Fig. 1). Figure 3 exhibits the results for the SLAB experiment. The PRESCRIBED experiment presents a very similar behavior.

3.2 Assimilating Pseudo-TRW Observations

3.2.1 SLAB and PRESCRIBED ocean

Here, we investigate two different experiments using SLAB and PRESCRIBED ocean conditions (see Table 1). Sensitivity experiments are conducted using the simple observation operator VSL-T to investigate the effect of using a SLAB ocean. This is motivated by the fact that the coupled ocean may lend predictability to the atmosphere as a slow component of the climate system. On the other hand, the climate of the PRESCRIBED experiment may follow the trends of the forced ocean conditions instead of the terrestrial proxy records. Therefore, the PRESCRIBED experiment's spread and error are expected to be smaller than the SLAB experiment. Figure 4 supports this hypothesis, showing a reduction in globally averaged free ensemble error in PRESCRIBED compared with the SLAB. Figure 4a illustrates that no error reduction is obtained for the forecast state. The expected value of the RMSE is slightly larger than the free ensemble simulation for both SLAB and PRESCRIBED. However, the analysis state has skill (Fig. 4b), especially prior to 1950s. The existence of the trend in the RMSE time-series may arise from cycling (reinitialization) of the ensemble or the choice of observation operator. The distribution density of the proxy record locations are biased to the Northern hemisphere; therefore, the error reduction of the analysis is more evident in the RMSE maps (Fig. 5).

The error reduction of the free ensemble run is modulated by the magnitude of the yearly internal variability of the particular variable at a specific site (compare figures 3 and 5). As a consequence, stations located in areas of strong yearly internal variability (i.e., Alaska) are more efficient than the others at reducing the error of the time-averaged state estimate. Additionally, more terrestrial records from the Southern Hemisphere may improve the state estimate (see Comboul et al. (2015) and the discussion at the end of this paper).

3.2.2 Minimum and Product Growth Rate Functions

Here, the performance of two different growth functions within the VSL's formulation, the product growth response (G_{Prod}) and the minimum growth response (G_{Min}), are investigated. In a simple DA experiment, AC15 have shown that the G_{Prod} performs slightly better than G_{Min}. As illustrated in figure 6a, the DA forecast presents no skill in the globally averaged temperature for both of the representations (VSL with Minimum t-norm (VSL-Min) and VSL-Prod). However, the use of VSL-Prod instead of VSL-Min appears beneficial to the filter performance for the analysis, as demonstrated in Figure 6b. The expected value of the RMSE shifts significantly toward lower values for VSL-Prod compared to the free ensemble run. The RMSE time-series shows an increasing trend for both VSL-Min and VSL-Prod. The RMSEs of DA forecasts using different VSL representations (figures 7a and 8a) do not indicate any improvement over the free ensemble run (Fig. 3b). The analysis of VSL-Prod performs slightly better skill than VSL-Min over Europe, the United States and Central Asia. Due to the strong nonlinear features of VSL-Min and VSL-Prod, the performance of these filters is expected to be degraded with respect to the ensemble runs constrained with VSL-T linear observation (see AC15). This behavior can be readily seen by comparing the figures 5b, 7b and 8b.

Our experiments show that the DA forecast has no skill over the free ensemble run. Therefore, using the forecast state of the free ensemble simulations we conduct an off-line DA to reconstruct the analysis state. The forecast of the free ensemble simulation at any individual year is used as the forecast state vector for that year. Following this methodology, the cycling step (reinitialization) of the ensemble is neglected. A very interesting feature of figure 9 is that the increasing trends in the RMSE time-series of the analysis have vanished. Figure 10 also confirms that the performance of off-line DA can compete with the performance of the online DA.

3.2.3 Signal to Noise Ratio

The Signal to Noise Ratio (SNR) is expressed as the ratio of the standard deviation of the nature (true) run to that of the additive white noise. We examined the performance of the off-line DA with different SNRs. Figure 11 exhibits that the time-averaged global RMSE shows an inflection point at values around $SNR = 1$ and reaches the error levels of a simulation without DA (free ensemble run) at $SNR = 0.03$, where all the pseudo-observations are ignored in the DA.

3.2.4 Time-Varying Soil Moisture

To investigate the effect of using the time-varying soil moisture fields instead of climatological average in DA approach, we implemented the Climate Prediction Center (CPC) Leaky Bucket Model (LBM) (Huang et al., 1996) in our DA code. The LBM code was extracted from VSL v2_3 (ftp://ftp.ncdc.noaa.gov/pub/data/paleo/softlib/vs-lite/). The precipitation and temperature output from SPEEDY is used as input for LBM to produce the time-varying soil moisture fields with inter-annual variations. In the next step we repeated the off-line data assimilation runs for two VSL presentations (VSL-Prod and VSL-Min) using the new soil moisture data. The results show that using the time-varying soil moisture fields has improved the error reduction of VSL-Min with minor improvement for VSL-Prod (Figures 12 and 13). The RMSE of VSL-Min reaches the one of VSL-Prod when using the soil moisture calculated from LBM. Figure 14 shows the boxplots of the RMSE time-series. The results show that while using the soil moisture calculated by the LBM improves the performance of the model for VSL-Min, the improvement in error reduction for VSL-Prod is not significant.

4 Discussion

Using the time-averaged EnKF methodology and a proxy forward model (VSL), we assimilated the pseudo-observations in an AGCM (SPEEDY). Using a set of perfect model experiments we studied two different aspects of DA, namely "on-line/off-line regime" and "on-line/off-line DA scheme". We concluded that the DA conducted here appears to be in the "off-line regime": while the analysis quantities have a significant skill, there is no skill for the forecast state. This result supports the studies of Huntley and Hakim (2010) and Pendergrass et al. (2012) who applied the time-averaged EnKF to a quasi-geostrophic atmospheric jet model. The appearance of the off-line regime can arise either from the dynamical model or from the DA scheme. Regarding the dynamical model, the main reason for losing skill in the forecast is that the period between consecutive observations exceeds the predictability horizon of the model. Under these conditions, as already discussed in AC15, the DA

ensemble spread reaches the spread of the free ensemble run before new observations are assimilated. For SPEEDY, due to its purely atmospheric nature, it is likely to have no forecast skill for a 1-year inter-observation period. Thus, it seems unlikely to improve the forecast skill using proxy records with yearly time resolution. However, there is already evidence for the existence of potential sources of climate internal variability with time scales longer than one year (Smith et al., 2012). The so called "annular modes" (Thompson and Wallace, 2000) may present internal variability in the high latitude areas. The latitudinal oscillation of the cell structure imposes variability at the fringes of the jet streams and oscillations of the ITCZ impacts the humidity (Holton and Hakim, 2013). ENSO affects a large portion of tropical and subtropical climate in time-scales larger than one year. Accordingly, we expect that it should be possible to obtain actual inter-annual predictability skill in the foreseeable future.

Regarding the DA scheme, a possible reason for the appearance of off-line regime is the time-averaged update strategy (Dirren and Hakim, 2005). It is not clear whether we can employ this technique with SPEEDY to properly estimate instantaneous quantities out of time averaged observations. In particular, it is not guaranteed that the time averaged and instantaneous variables are de-correlated.

Given that our DA simulation is in the off-line regime (no forecast skill), we have conducted an "off-line DA" (no-cycling) for two different representations of VSL forward model. Despite its lack of accumulation of observational information over time, off-line DA has already been shown to be more robust than traditional Climate Field Reconstruction (CFR) techniques based on orthogonal empirical functions and stationarity assumptions (Steiger et al., 2014; Hakim et al., 2016). Our off-line DA experiments support the results obtained by the two-scale Lorenz (1996) model (AC15) regarding the influence of the PLF representation on the filter performance. The efficacy of the EnKF-based time averaged state estimation strategy appeared to be significantly sensitive to the selection of the t-norm used to calculate the growth rate. For the off-line DA presented here, the product t-norm (VSL-Prod) outperforms the minimum t-norm (VSL-Min) which is used in the original formulation of VSL forward model. Tolwinski-Ward et al. (2014) described trees as fundamentally lossy[1] recorders of climate, due to the integrated nature of the information contained in them and the standardization process used to minimize the non-climatic effects on growth. Growth is influenced by temperature and/or moisture and the transitions between limitation regimes may happen suddenly ("abrupt shifting") (Acevedo et al., 2015). In the same vein, we argue that the "abrupt shifting" of recorded variable (temperature or moisture)–implied by the minimum function used in VSL's original formulation– might constitute an additional source of lossyness. We conclude that this can be substantially reduced by resorting to alternative Fuzzy Logic-based representations of the PLF.

As a cautionary remark, we want to highlight the several important limitations of the experiments described in this paper. The generated pseudo-TRW observations lack a threshold for temperature or moisture after which the growth response does not change and their contamination with noise was performed assuming optimistically high SNR levels. Furthermore, the response thresholds were set in a completely homogeneous fashion for all the observational stations, whereas actual TRW networks are strongly heterogeneous in that sense, comprising chronologies generated under highly dissimilar growth limitation

---

[1]This adjective is currently used in the information technology area to designate data encoding methods that lead to information loss from the original version for the sake of reducing the amount of data needed to store the content.

regimes. Additionally, the efficiency of EnKF technique used relies on the Gaussianity of all the variables of the model. Nevertheless, in a climate model some variables can present strongly non-Gaussian properties –specially definite positive quantities such as humidity– and their estimation should in principle be performed with more sophisticated strategies such a Gaussian anamorphosis (Bocquet et al., 2010; Lien et al., 2013). It is worth mentioning the necessity of explicitly addressing

5   model errors by conducting imperfect model OSSE. It is important to emphasize that the OSSE presented in this manuscript represents the first step of the long hierarchy of DA experiments to achieve an effective assimilation of proxy records into climate models using forward proxy models. We encourage further experiments using comprehensive earth system models with longer time scale processes to bring the proxy DA into an online regime. However, assimilation of proxies in an earth system model with different components may lead to inter-component DA pollutions and is computationally very expensive.

10   *Acknowledgements.* This work was supported by German Federal Ministry of Education and Research (BMBF) as Research for Sustainability initiative (FONA); www.fona.de through PalMod project (FKZ: 01LP1511A). The computational resources were made available by the High Performance Computing Center (ZEDAT) at Freie Universität Berlin and the German Climate Computing Center (DKRZ). W.A. wishes to acknowledge partial financial support by the Helmholtz graduate research school GEOSIM.

References

Acevedo, W., Reich, S., and Cubasch, U.: Towards the assimilation of tree-ring-width records using ensemble Kalman filtering techniques, Climate Dynamics, pp. 1–12–, http://dx.doi.org/10.1007/s00382-015-2683-1, 2015.

Amezcua, J., Ide, K., Kalnay, E., and Reich, S.: Ensemble transform Kalman-Bucy filters, Q.J.R. Meteorol. Soc., 140, 995–1004, http://dx.doi.org/10.1002/qj.2186, 2014.

Annan, J. D. and Hargreaves, J. C.: Identification of climatic state with limited proxy data, Clim. Past, 8, 1141–1151, http://www.clim-past.net/8/1141/2012/, 2012.

Barkmeijer, J., Iversen, T., and Palmer, T. N.: Forcing singular vectors and other sensitive model structures, Quarterly Journal of the Royal Meteorological Society, 129, 2401–2423, doi:10.1256/qj.02.126, http://dx.doi.org/10.1256/qj.02.126, 2003.

Bhend, J., Franke, J., Folini, D., Wild, M., and Brönnimann, S.: An ensemble-based approach to climate reconstructions, Clim. Past, 8, 963–976, http://www.clim-past.net/8/963/2012/, 2012.

Bocquet, M., Pires, C. A., and Wu, L.: Beyond Gaussian Statistical Modeling in Geophysical Data Assimilation, Mon. Wea. Rev., 138, 2997–3023, http://dx.doi.org/10.1175/2010MWR3164.1, 2010.

Boucher, E., Guiot, J., Hatté, C., Daux, V., Danis, P.-A., and Dussouillez, P.: An inverse modeling approach for tree-ring-based climate reconstructions under changing atmospheric CO_2 concentrations, Biogeosciences, 11, 3245–3258, http://www.biogeosciences.net/11/3245/2014/, 2014.

Breitenmoser, P., Brönnimann, S., and Frank, D.: Forward modelling of tree-ring width and comparison with a global network of tree-ring chronologies, Clim. Past, 10, 437–449, http://www.clim-past.net/10/437/2014/, 2014.

Brönnimann, S.: Towards a paleoreanalysis?, ProClim-Flash, 1, 16, 2011.

Burgers, G., van Leeuwen, P. J., and Evensen, G.: Analysis scheme in the ensemble Kalman filter, Monthly Weather Review, 126, 1719–1724, http://dx.doi.org/10.1029/94JC00572, 1998.

Comboul, M., Emile-Geay, J., Hakim, G. J., and Evans, M. N.: Paleoclimate Sampling as a Sensor Placement Problem, J. Climate, 28, 7717–7740, doi:10.1175/JCLI-D-14-00802.1, http://dx.doi.org/10.1175/JCLI-D-14-00802.1, 2015.

Crucifix, M.: Traditional and novel approaches to palaeoclimate modelling, Quaternary Science Reviews, 57, 1–16, http://www.sciencedirect.com/science/article/pii/S0277379112003472, 2012.

Dee, S. G., Steiger, N. J., Emile-Geay, J., and Hakim, G. J.: On the utility of proxy system models for estimating climate states over the common era, J. Adv. Model. Earth Syst., pp. n/a–n/a, http://dx.doi.org/10.1002/2016MS000677, 2016.

Deza, J. I., Masoller, C., and Barreiro, M.: Distinguishing the effects of internal and forced atmospheric variability in climate networks, Nonlin. Processes Geophys., 21, 617–631, http://www.nonlin-processes-geophys.net/21/617/2014/, 2014.

Dirren, S. and Hakim, G. J.: Toward the assimilation of time-averaged observations, Geophysical Research Letters, 32, L04 804, doi:10.1029/2004GL021444, http://dx.doi.org/10.1029/2004GL021444, 2005.

Dubinkina, S. and Goosse, H.: An assessment of particle filtering methods and nudging for climate state reconstructions, Climate of the Past, 9, 1141–1152, doi:10.5194/cp-9-1141-2013, http://www.clim-past.net/9/1141/2013/, 2013.

Dubinkina, S., Goosse, H., Sallaz-Damaz, Y., Crespin, E., and Crucifix, M.: Testing a particle filter to reconstruction climate over the past centuries, Int. J. Bifurcation Chaos, 21, 3611–3618, doi:10.1142/S0218127411030763, http://dx.doi.org/10.1142/S0218127411030763, 2011.

Evans, M., Tolwinski-Ward, S., Thompson, D., and Anchukaitis, K.: Applications of proxy system modeling in high resolution paleoclimatology, Quaternary Science Reviews, 76, 16 – 28, doi:http://dx.doi.org/10.1016/j.quascirev.2013.05.024, http://www.sciencedirect.com/science/article/pii/S0277379113002011, 2013.

Evensen, G.: Sequential data assimilation with a nonlinear quasi-geostrophic model using Monte Carlo methods to forecast error statistics, Journal of Geophysical Research: Oceans, 99, 10 143–10 162, doi:10.1029/94JC00572, http://dx.doi.org/10.1029/94JC00572, 1994.

Fritts, H. C.: Tree rings and climate, Academic Press, New York, 1976.

Gibson, J. K., Kållberg, P., Uppala, S., Nomura, A., Hernandez, A., and Serrano, E.: ERA Description, in: ECMWF ERA-15 Project Report Series, No. 1, European Centre for Medium-Range Weather Forecasts, Shinfield, Reading, UK, 1997.

Hakim, G., Annan, J., Broennimann, S., Crucifix, M., Edwards, T., Goosse, H., Paul, A., van der Schrier, G., and Widmann, M.: Overview of data assimilation methods, PAGES, 21, 2013.

Hakim, G. J., Emile-Geay, J., Steig, E. J., Noone, D., Anderson, D. M., Tardif, R., Steiger, N., and Perkins, W. A.: The last millennium climate reanalysis project: Framework and first results, J. Geophys. Res. Atmos., 121, 6745–6764, http://dx.doi.org/10.1002/2016JD024751, 2016.

Hamill, T. M.: Ensemble-based atmospheric data assimilation, in: Predictability of Weather and Climate, edited by Palmer, T. and Hagedorn, R., Cambridge University Press, web: http://dx.doi.org/10.1017/CBO9780511617652.007, 2006.

Herceg Bulić, I. and Kucharski, F.: Delayed ENSO impact on spring precipitation over North/Atlantic European region, Climate Dynamics, 38, 2593–2612, http://dx.doi.org/10.1007/s00382-011-1151-9, 2012.

Holton, J. and Hakim, G. J.: An Introduction to Dynamic Meteorology, Academic Press, http://books.google.de/books?id=hLQRAQAAIAAJ, 2013.

Huang, J., van den Dool, H. M., and Georgarakos, K. P.: Analysis of Model-Calculated Soil Moisture over the United States (1931-1993) and Applications to Long-Range Temperature Forecasts, J. Climate, 9, 1350–1362, doi:10.1175/1520-0442(1996)009<1350:AOMCSM>2.0.CO;2, http://dx.doi.org/10.1175/1520-0442(1996)009<1350:AOMCSM>2.0.CO;2, 1996.

Hughes, M. and Ammann, C.: The future of the past – an earth system framework for high resolution paleoclimatology: editorial essay, Climatic Change, 94, 247–259, doi:10.1007/s10584-009-9588-0, http://dx.doi.org/10.1007/s10584-009-9588-0, 2009.

Hughes, M., Guiot, J., and Ammann, C.: An emerging paradigm: Process-based climate reconstructions, PAGES news, 18, 87–89, 2010.

Hunt, B. R., Kostelich, E. J., and Szunyogh, I.: Efficient data assimilation for spatiotemporal chaos: A local ensemble transform Kalman filter, Physica D: Nonlinear Phenomena, 230, 112–126, http://www.sciencedirect.com/science/article/pii/S0167278906004647, 2007.

Huntley, H. and Hakim, G.: Assimilation of time-averaged observations in a quasi-geostrophic atmospheric jet model, 35, 995–1009–, http://dx.doi.org/10.1007/s00382-009-0714-5, 2010.

Kalman, R. E.: A New Approach to Linear Filtering and Prediction Problems, Transactions of the ASME–Journal of Basic Engineering, 82, 35–45, 1960.

Kalnay, E.: Atmospheric modeling, data assimilation, and predictability, Cambridge university press, 2003.

Kurahashi-Nakamura, T., Losch, M., and Paul, A.: Can sparse proxy data constrain the strength of the Atlantic meridional overturning circulation?, Geoscientific Model Development, 7, 419–432, doi:10.5194/gmd-7-419-2014, http://www.geosci-model-dev.net/7/419/2014/, 2014.

Lahoz, W., Khattatov, B., and Menard, R.: Data Assimilation: Making Sense of Observations, Springer, http://books.google.de/books?id=KivkFpthm1EC, 2010.

Li, H., Kalnay, E., Miyoshi, T., and Danforth, C. M.: Accounting for Model Errors in Ensemble Data Assimilation, Mon. Wea. Rev., 137, 3407–3419, http://dx.doi.org/10.1175/2009MWR2766.1, 2009.

Lien, G.-Y., Kalnay, E., and Miyoshi, T.: Effective assimilation of global precipitation: simulation experiments, 2013, 65, http://www.tellusa.net/index.php/tellusa/article/view/19915, 2013.

Lorenc, A. C.: Analysis methods for numerical weather prediction, Q.J.R. Meteorol. Soc., 112, 1177–1194, http://dx.doi.org/10.1002/qj.49711247414, 1986.

5 Lorenz, E. N.: Predictability, a problem partly solved, in: Proceedings of ECMWF seminar on Predictability, pp. 1–19, ECMWF, Reading, UK, 1996.

Marchini, A.: Modelling Ecological Processes with Fuzzy Logic Approaches, in: Modelling Complex Ecological Dynamics, edited by Jopp, F., Reuter, H., and Breckling, B., pp. 133–145, Springer Berlin Heidelberg, 2011.

Mathiot, P., Goosse, H., Crosta, X., Stenni, B., Braida, M., Renssen, H., Van Meerbeeck, C. J., Masson-Delmotte, V., Mairesse, A., and

10 Dubinkina, S.: Using data assimilation to investigate the causes of Southern Hemisphere high latitude cooling from 10 to 8 ka BP, Climate of the Past, 9, 887–901, doi:10.5194/cp-9-887-2013, http://www.clim-past.net/9/887/2013/, 2013.

Matsikaris, A., Widmann, M., and Jungclaus, J.: On-line and off-line data assimilation in palaeoclimatology: a case study, Clim. Past, 11, 81–93, http://www.clim-past.net/11/81/2015/, 2015.

McShane, B. B. and Wyner, A. J.: A Statistical Analysis of Multiple Temperature Proxies: Are Reconstructions of Surface Temperatures

15 Over the Last 1000 Years Reliable?, Annals of Applied Statistics, 5, 5–44, doi:10.1214/10-AOAS398, 2011.

Miyoshi, T.: Ensemble Kalman filter experiments with a primitive-equation global model, Ph.D. thesis, University of Maryland, College Park, 197pp., 2005.

Miyoshi, T.: The Gaussian Approach to Adaptive Covariance Inflation and Its Implementation with the Local Ensemble Transform Kalman Filter, Mon. Wea. Rev., 139, 1519–1535, http://dx.doi.org/10.1175/2010MWR3570.1, 2010.

20 Molteni, F.: Atmospheric simulations using a GCM with simplified physical parametrizations. I: model climatology and variability in multi-decadal experiments, 20, 175–191–, http://dx.doi.org/10.1007/s00382-002-0268-2, 2003.

Nguyen, H. T., Prasad, N. R., Walker, C. L., and Walker, E. A.: A First Course in Fuzzy and Neural Control, Chapman and Hall/CRC, 1 edn., 2002.

Paul, A. and Schäfer-Neth, C.: How to combine sparse proxy data and coupled climate models, Quaternary Science Reviews, 24, 1095–1107,

25 http://www.sciencedirect.com/science/article/pii/S0277379104002239, 2005.

Pendergrass, A., Hakim, G., Battisti, D., and Roe, G.: Coupled Air-Mixed Layer Temperature Predictability for Climate Reconstruction, Journal of Climate, 25, 459–472, doi:10.1175/2011JCLI4094.1, http://dx.doi.org/10.1175/2011JCLI4094.1, 2012.

Reich, S. and Cotter, C.: Probabilistic Forecasting and Bayesian Data Assimilation, Cambridge University Press, https://books.google.de/books?id=xVpiCAAAQBAJ, 2015.

30 Ruiz, J. J., Pulido, M., and Miyoshi, T.: Estimating Model Parameters with Ensemble-Based Data Assimilation: A Review, Journal of the Meteorological Society of Japan. Ser. II, 91, 79–99, doi:10.2151/jmsj.2013-201, 2013.

Salski, A.: Ecological Applications of Fuzzy Logic, in: Ecological Informatics, edited by Recknagel, F., pp. 3–14, Springer Berlin Heidelberg, 2006.

Schneider, T., Bischoff, T., and Haug, G. H.: Migrations and dynamics of the intertropical convergence zone, Nature, 513, 45–53, http:

35 //dx.doi.org/10.1038/nature13636, 2014.

Se, Z.: Fuzzy Logic and Hydrological Modeling, CRC Press, 2009.

Smith, D. M., Scaife, A. A., and Kirtman, B. P.: What is the current state of scientific knowledge with regard to seasonal and decadal forecasting?, Environmental Research Letters, 7, 015 602, http://stacks.iop.org/1748-9326/7/i=1/a=015602, 2012.

Smith, T. M., Reynolds, R. W., Peterson, T. C., and Lawrimore, J.: Improvements to NOAA's Historical Merged Land-Ocean Surface Temperature Analysis (1880-2006), J. Climate, 21, 2283–2296, doi:10.1175/2007JCLI2100.1, http://dx.doi.org/10.1175/2007JCLI2100.1, 2008.

Steiger, N., Hakim, G., Steig, E., Battisti, D., and Roe, G.: Assimilation of Time-Averaged Pseudoproxies for Climate Reconstruction, Journal of Climate, 27, 426–441, doi:10.1175/JCLI-D-12-00693.1, http://dx.doi.org/10.1175/2011JCLI4094.1, 2014.

5   Talagrand, O.: Assimilation of observations, an introduction, Journal-Meteorological Society of Japan Series 2, 75, 81–99, 1997.

Thompson, D. W. J. and Wallace, J. M.: Annular Modes in the Extratropical Circulation. Part I: Month-to-Month Variability, J. Climate, 13, 1000–1016, http://dx.doi.org/10.1175/1520-0442(2000)013<1000:AMITEC>2.0.CO;2, 2000.

Tippett, M. K., Anderson, J. L., Bishop, C. H., Hamill, T. M., and Whitaker, J. S.: Ensemble Square Root Filters*, Mon. Wea. Rev., 131, 1485–1490, http://dx.doi.org/10.1175/1520-0493(2003)131<1485:ESRF>2.0.CO;2, 2003.

10   Tolwinski-Ward, S., Tingley, M., Evans, M., Hughes, M., and Nychka, D.: Probabilistic reconstructions of local temperature and soil moisture from tree-ring data with potentially time-varying climatic response, Climate Dynamics, pp. 1–16, doi:10.1007/s00382-014-2139-z, http://dx.doi.org/10.1007/s00382-014-2139-z, 2014.

Tolwinski-Ward, S. E.: Inference on Tree-Ring Width and Paleoclimate Using a Proxy Model of Intermediate Complexity, Ph.D. thesis, The University of Arizona, http://hdl.handle.net/10150/241975, 2012.

15   Tolwinski-Ward, S. E., Evans, M. N., Hughes, M., and Anchukaitis, K. J.: An efficient forward model of the climate controls on interannual variation in tree-ring width, Climate Dynamics, 36, 2419–2439, doi:10.1007/s00382-010-0945-5, http://dx.doi.org/10.1007/s00382-010-0945-5, 2011.

Vaganov, E., Hughes, M., and Shashkin, A.: Growth Dynamics of Conifer Tree Rings: Images of Past and Future Environments, vol. 183 of *Ecological studies*, Springer, New York, 2006.

20   van der Schrier, G. and Barkmeijer, J.: Bjerknes' hypothesis on the coldness during AD 1790-1820 revisited, Climate Dynamics, 25, 537–553–, http://dx.doi.org/10.1007/s00382-005-0053-0, 2005.

Van Leeuwen, P. J., Cheng, Y., and Reich, S.: Nonlinear data assimilation, Springer, 2015.

von Storch, H., Cubasch, U., González-Ruoco, J., Jones, J., Widmann, M., and Zorita, E.: Combining paleoclimatic evidence and GCMs by means of Data Assimilation Through Upscaling and Nudging (DATUN), Proceedings 28-31. 11th Symposium on global change studies, 25   AMS, Long Beach, CA, USA.9-14/1, pp. 2119–2128, 2000.

Whitaker, J. S., Compo, G. P., and Thépaut, J.-N.: A Comparison of Variational and Ensemble-Based Data Assimilation Systems for Reanalysis of Sparse Observations, Mon. Wea. Rev., 137, 1991–1999, http://dx.doi.org/10.1175/2008MWR2781.1, 2009.

Widmann, M., Goosse, H., van der Schrier, G., Schnur, R., and Barkmeijer, J.: Using data assimilation to study extratropical Northern Hemisphere climate over the last millennium, Climate of the Past, 6, 627–644, doi:10.5194/cp-6-627-2010, http://www.clim-past.net/6/30   627/2010/, 2010.

Woollings, T., Pinto, J. G., and Santos, J. A.: Dynamical Evolution of North Atlantic Ridges and Poleward Jet Stream Displacements, J. Atmos. Sci., 68, 954–963, http://dx.doi.org/10.1175/2011JAS3661.1, 2011.

Xue, Y., Smith, T. M., and Reynolds, R. W.: Interdecadal Changes of 30-Yr SST Normals during 1871-2000, J. Climate, 16, 1601–1612, doi:10.1175/1520-0442(2003)016<1601:ICOYSN>2.0.CO;2, http://journals.ametsoc.org/doi/abs/10.1175/1520-0442%282003%29016%35   3C1601%3AICOYSN%3E2.0.CO%3B2, 2003.

Zadeh, L. A.: Fuzzy logic and approximate reasoning, Synthese, 30, 407–428, 1975.
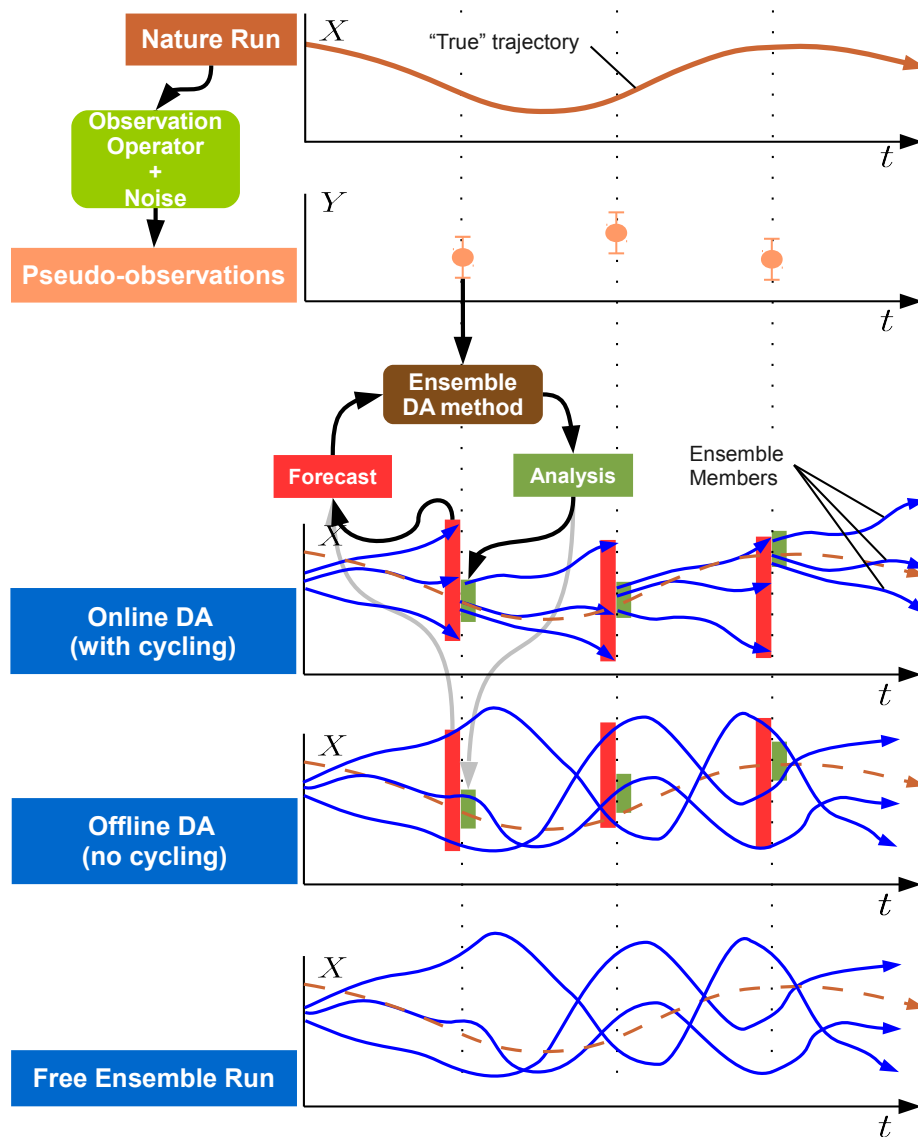
Figure 1. Schematic of a typical Observation System Simulation Experiment (OSSE) with ensemble "online" (with cycling) and "offline" (no-cycling) DA methods. t designates the time axis and $X(Y)$ denotes the model state (observation) space. Sharp (rounded) cornered boxes represent data (processes). Red (green) vertical shadings indicate the *Forecast* (*Analysis*) spread. Vertical dotted lines represent the assimilation steps.
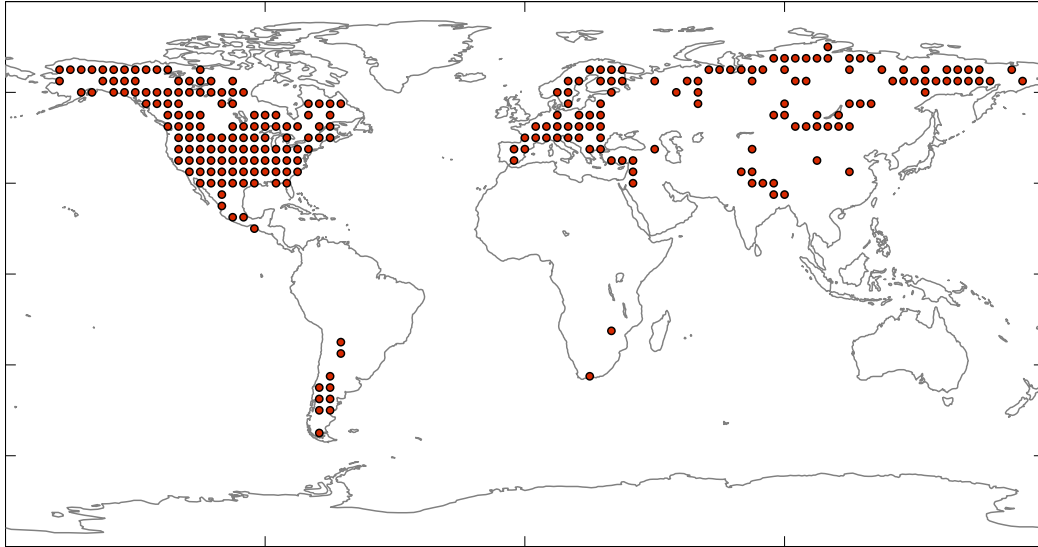
Figure 2. Station set resembling real TRW network from Breitenmoser et al. (2014)

Table 1. Runs' characteristics.

No.	1	2	3	4
Forward Model	VSL-T	VSL-T	VSL-Min	VSL-Prod
Ocean	*SLAB*	*PRESCRIBED*	*SLAB*	*SLAB*

Simulations are 150 years long.

a) Free ensemble Spread
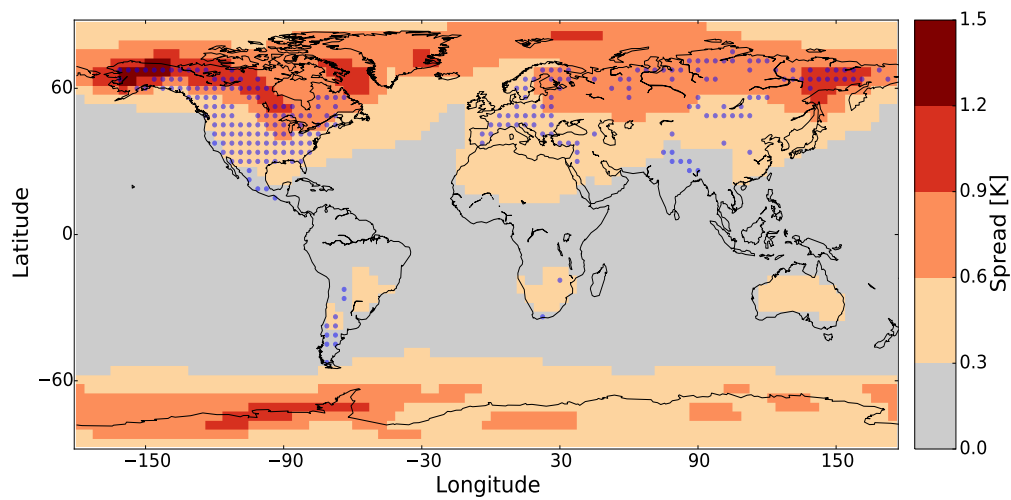
b) Free ensemble Error
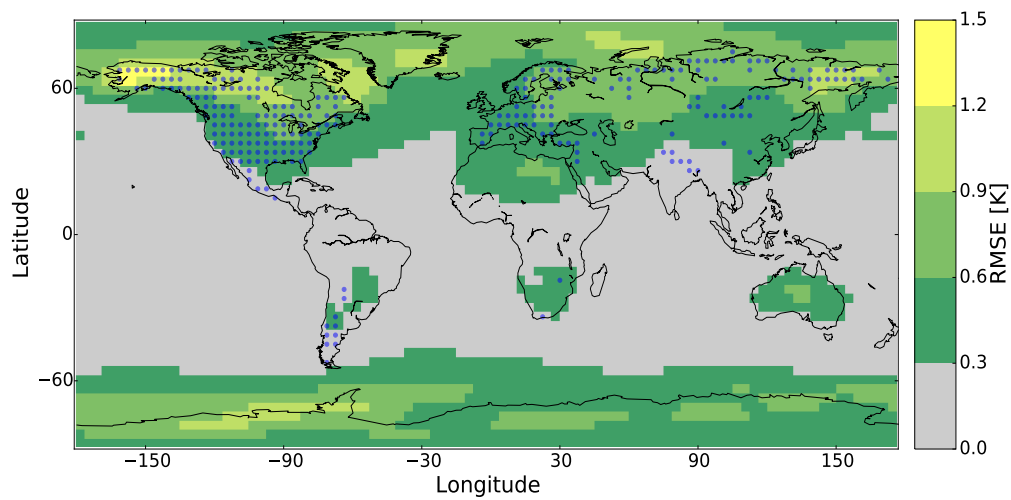
Figure 3. Free ensemble simulations for the SLAB experiment: a) Ensemble Spread [K] of near surface temperatures, b) Free ensemble RMSE [K].

a)

b)
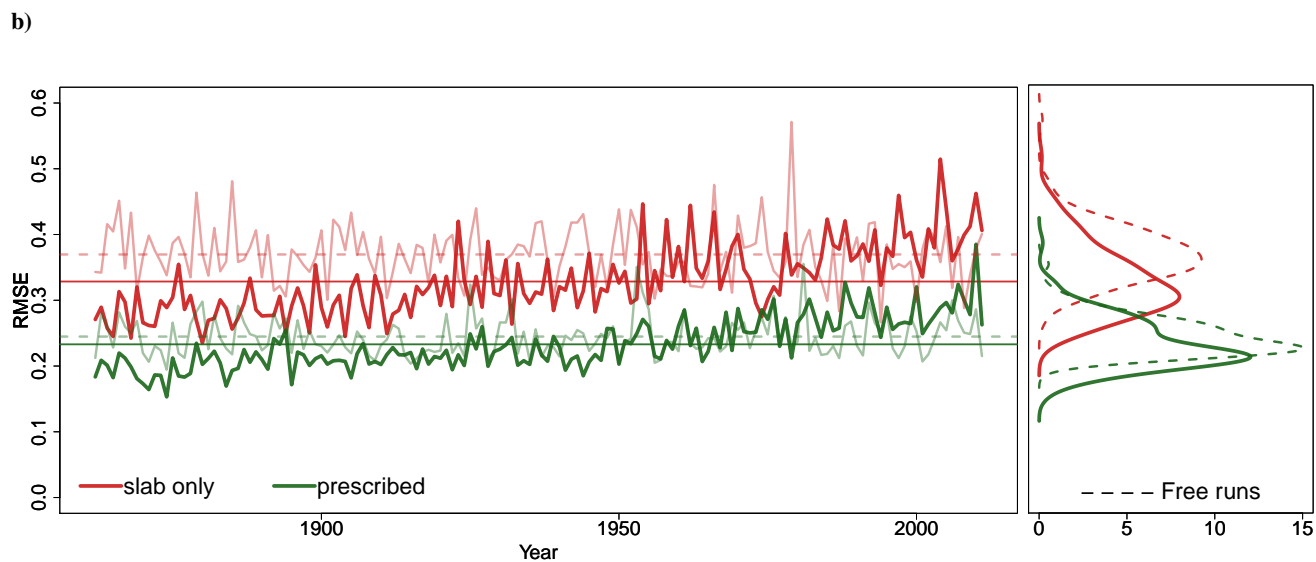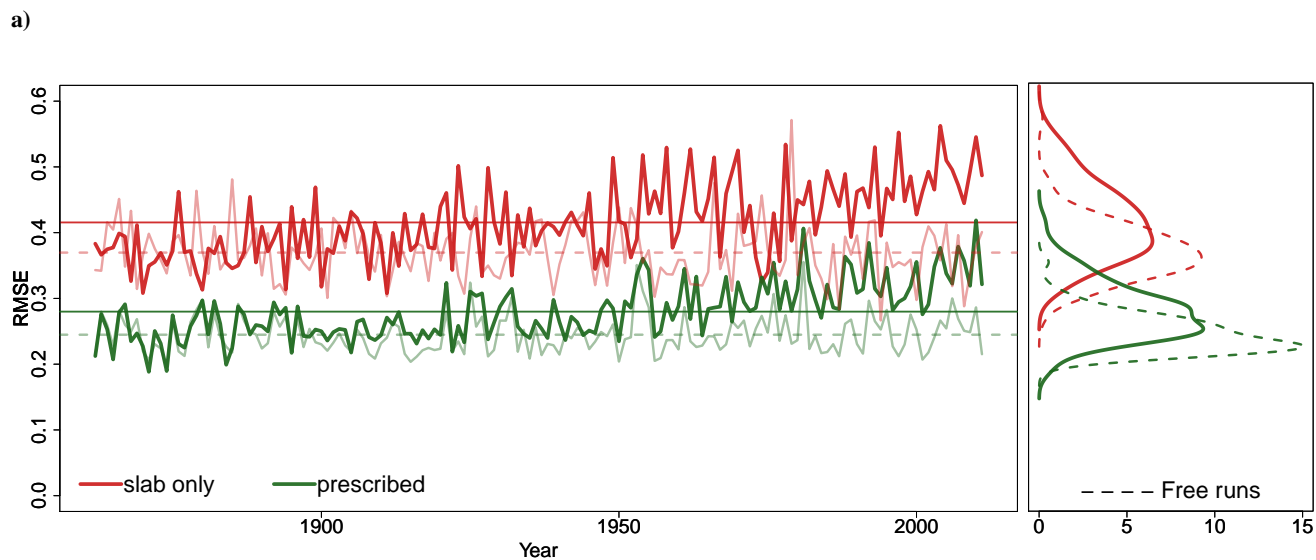
Figure 4. Global ensemble mean for a) Forecast constrained by VSL-T pseudo-TRW observations (bold lines) and Free run (thin lines); b) Analysis (solid lines) and Free run (thin lines). Horizontal lines exhibit the mean values. Right panels exhibit the histograms of the time-series.

a) DA forecast for VSL-T
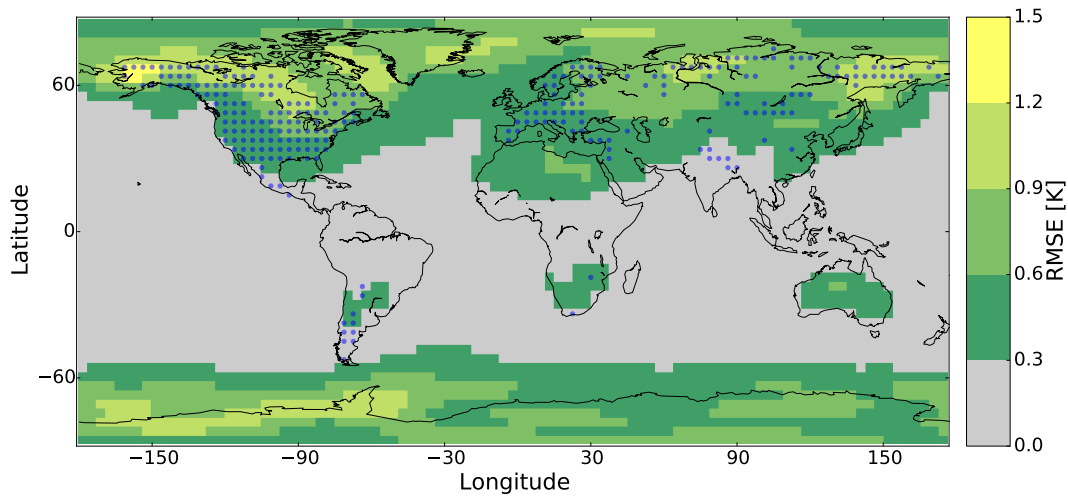
b) DA analysis for VSL-T
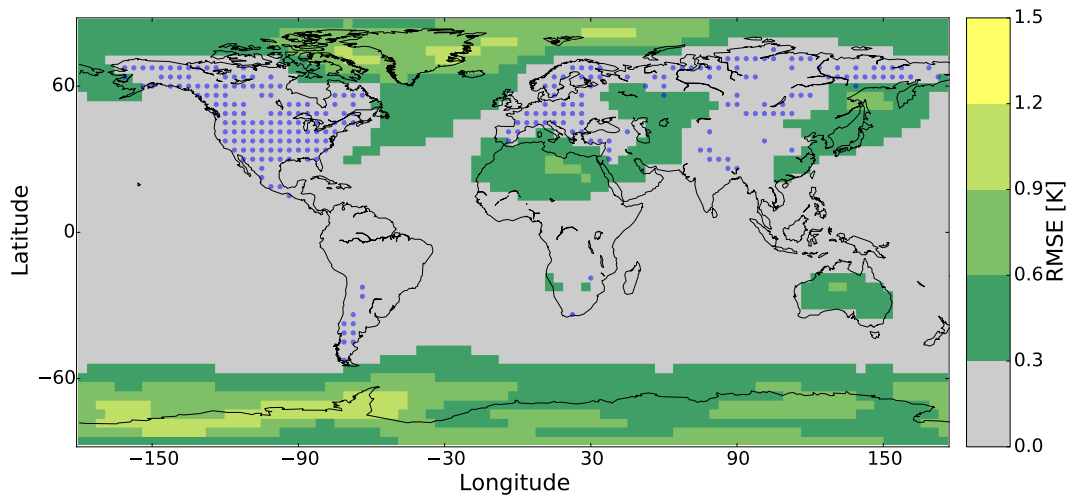
Figure 5. Time-averaged RMSEs of SLAB experiment for a) DA forecast and b) DA analysis using the VSL-T observation operator.
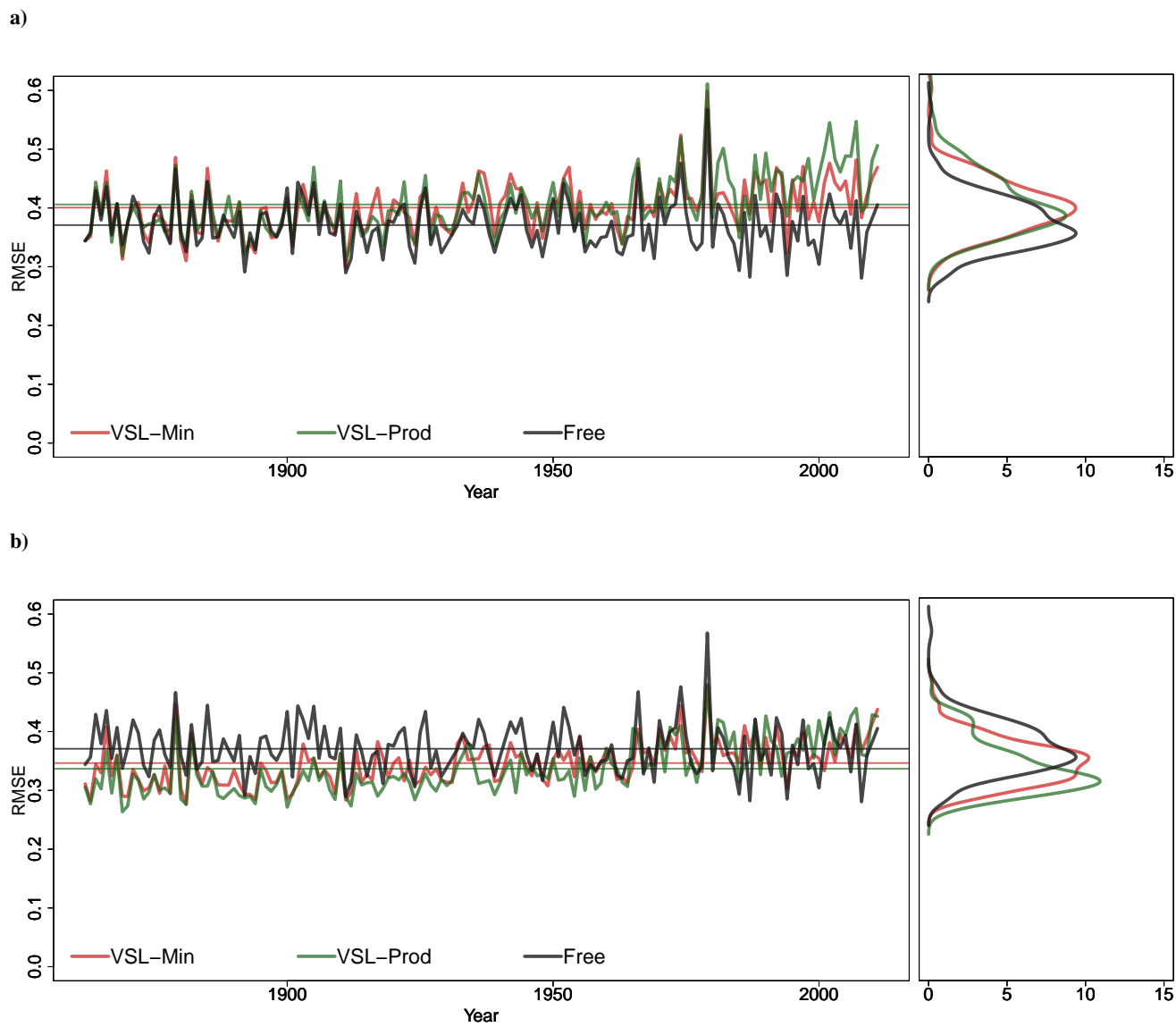
Figure 6. Global ensemble mean for a) forecast and b) analysis constrained by VSL-Min (red) and VSL-Prod (green) pseudo-TRW observations and free run (black). Horizontal lines exhibit the mean values. Right panels exhibit the histograms of the time-series.

a) DA forecast for VSL-Min
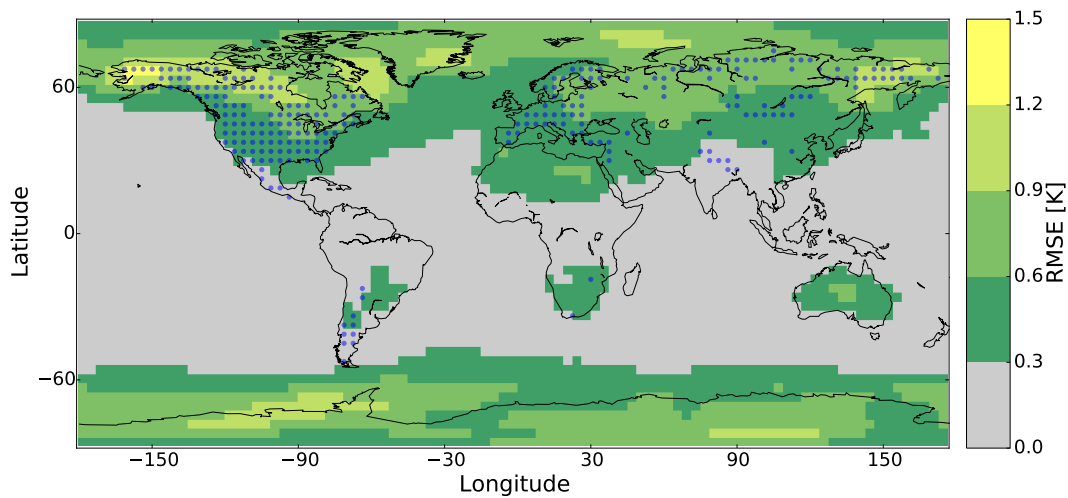
b) DA analysis for VSL-Min
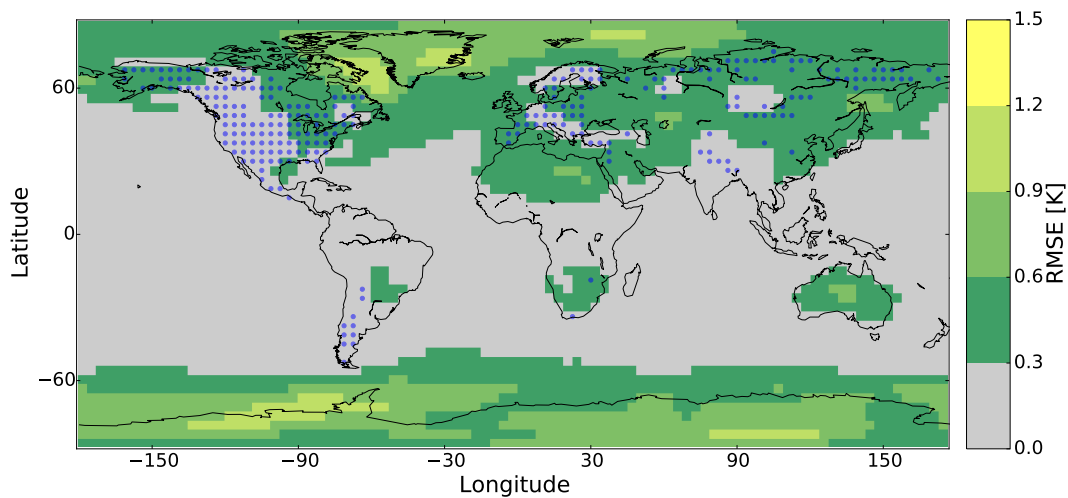
Figure 7. Time-averaged RMSEs of SLAB experiment for a) DA forecast and b) DA analysis using the VSL-Min observation operator.

a) DA forecast for VSL-Prod
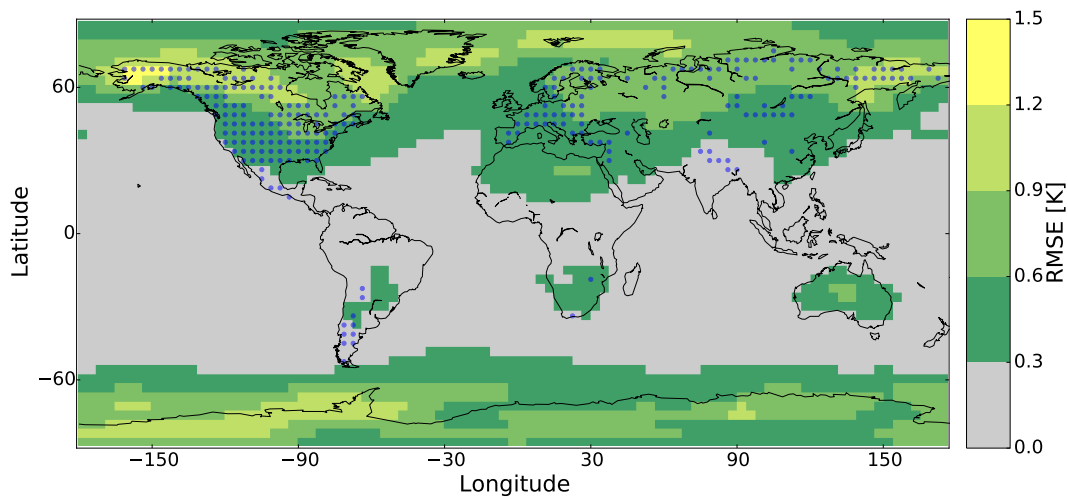
b) DA analysis for VSL-Prod
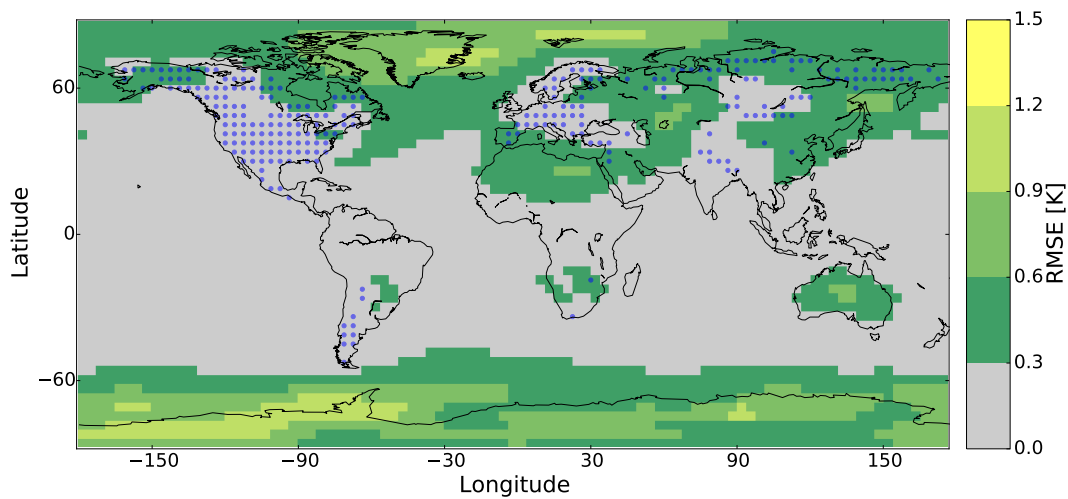
Figure 8. Time-averaged RMSEs of SLAB experiment for a) DA forecast and b) DA analysis using the VSL-Prod observation operator.
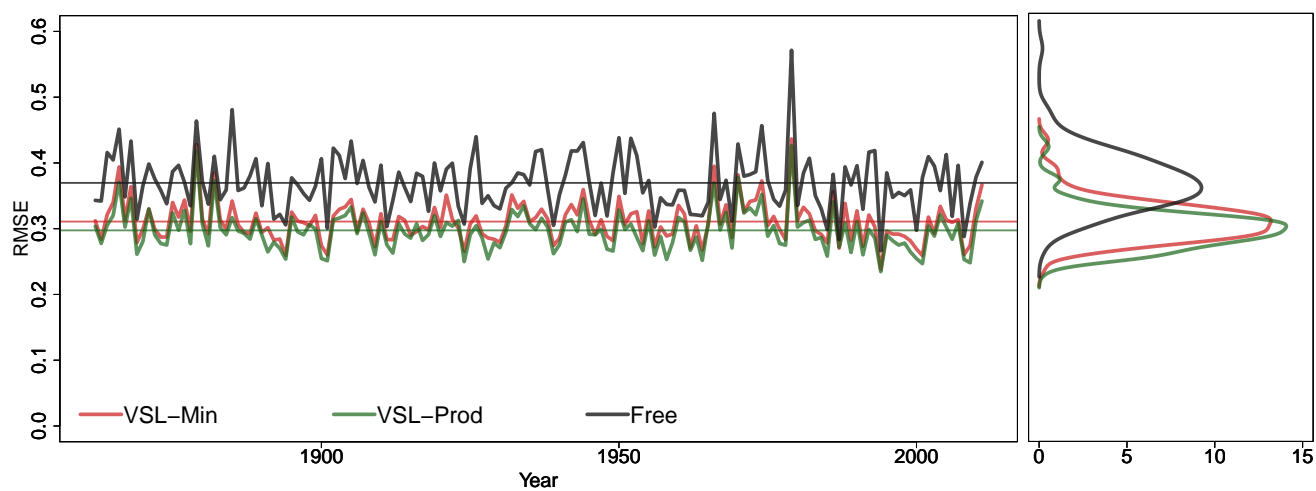
Figure 9. Global ensemble mean for analysis constrained by VSL-Min (red) and VSL-Prod (green) pseudo-TRW observations and free run (black). Horizontal lines exhibit the mean values. Right panel exhibits the histograms of the time-series.

a) DA analysis for VSL-Min with nocycling
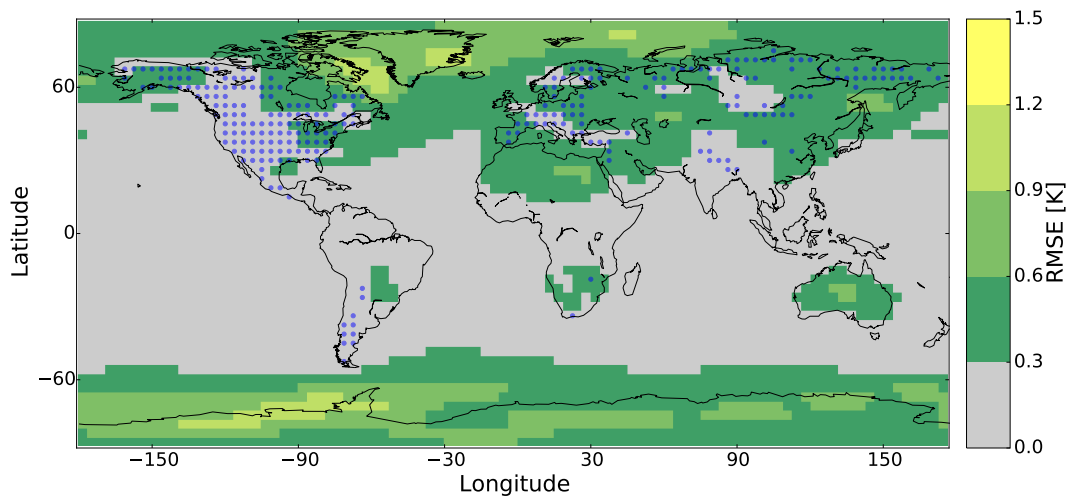
b) DA analysis for VSL-Prod with nocycling
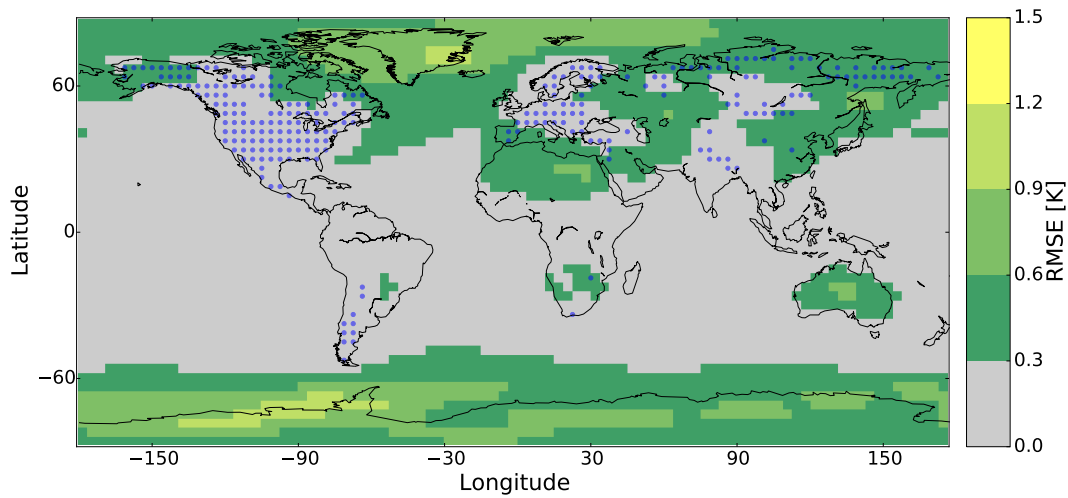
Figure 10. Time-averaged RMSEs of SLAB experiment for a) nocycling DA analysis using the VSL-Min and b) the VSL-Prod observation operator.
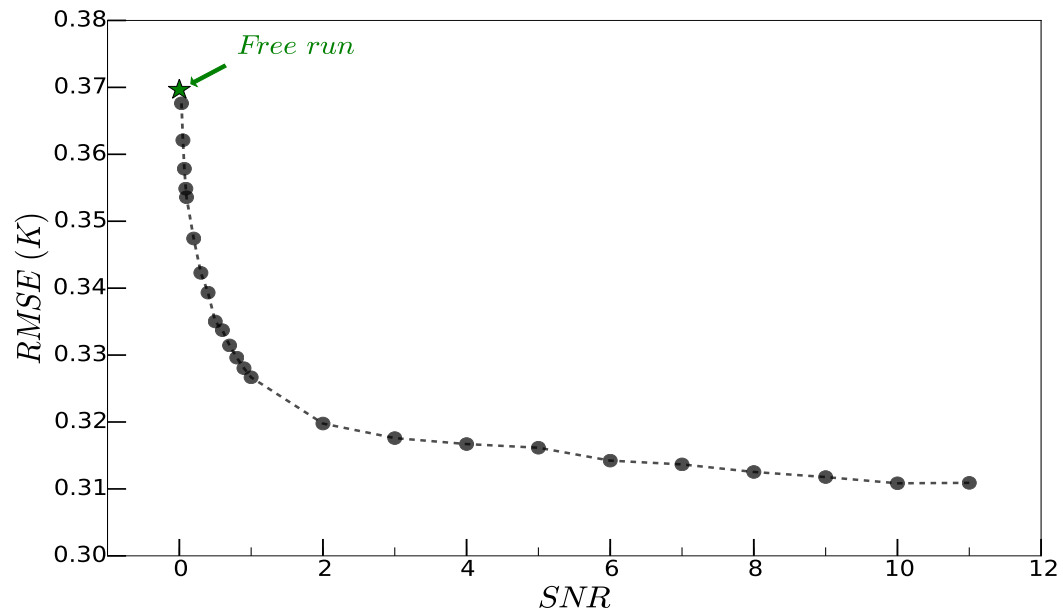
Figure 11. Time-averaged global RMSEs of SLAB experiment for nocycling DA using the VSL-Min and different signal to noise ratios. The Green star shows the Free run RMSE.

a)

b)
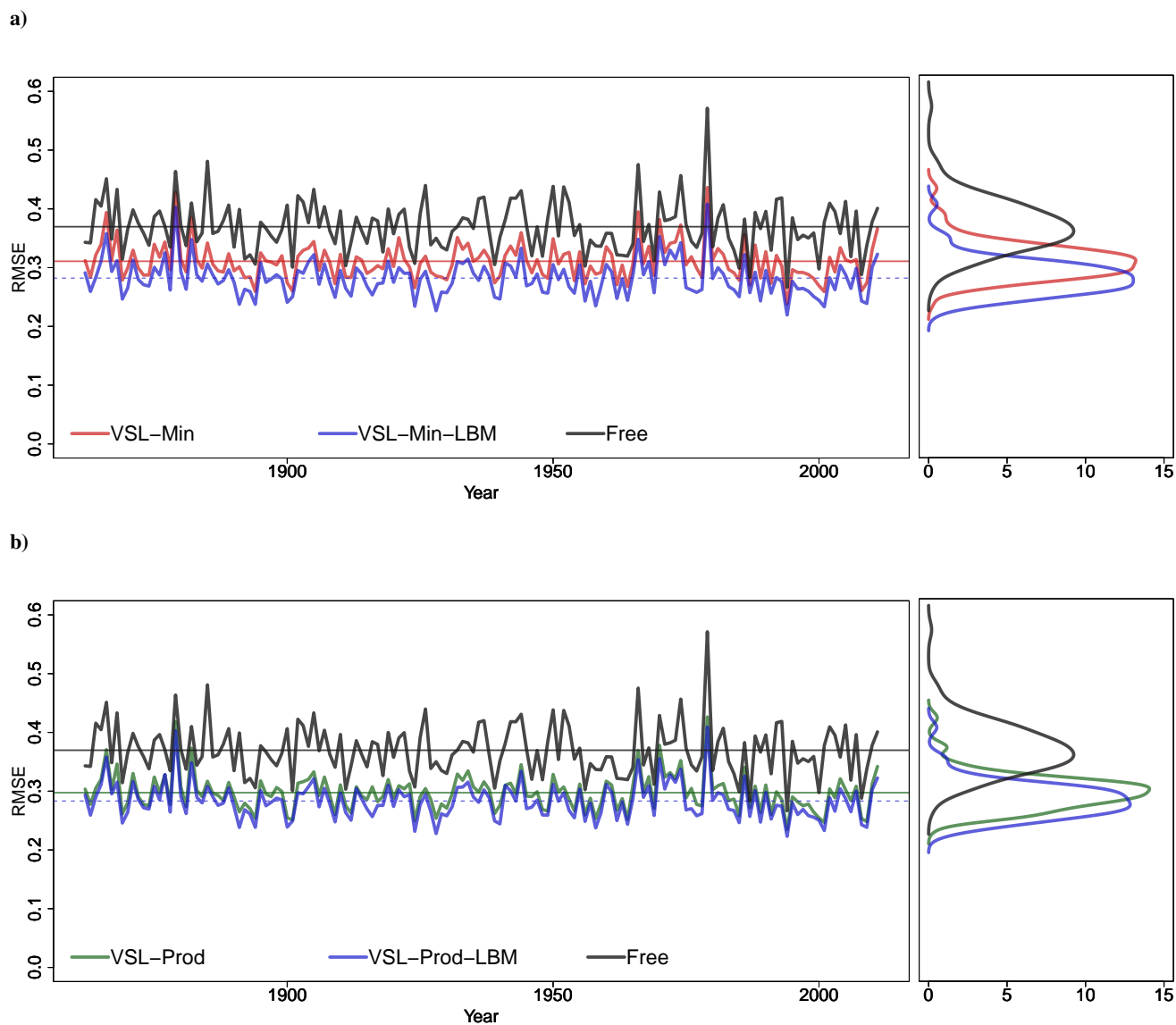
Figure 12. Global ensemble mean for analysis constrained by pseudo-TRW observations for a) VSL-Min with the climatological soil moisture (red), with the soil moisture computed by Leaky Bucket Model (blue) and free run (black); b) VSL-Prod with the climatological soil moisture (green), with the soil moisture computed by Leaky Bucket Model (blue) and free run (black). Horizontal lines exhibit the mean values. Right panels exhibit the histograms of the time-series.

a) DA analysis for VSL-Min with Leaky Bucket Model and nocycling
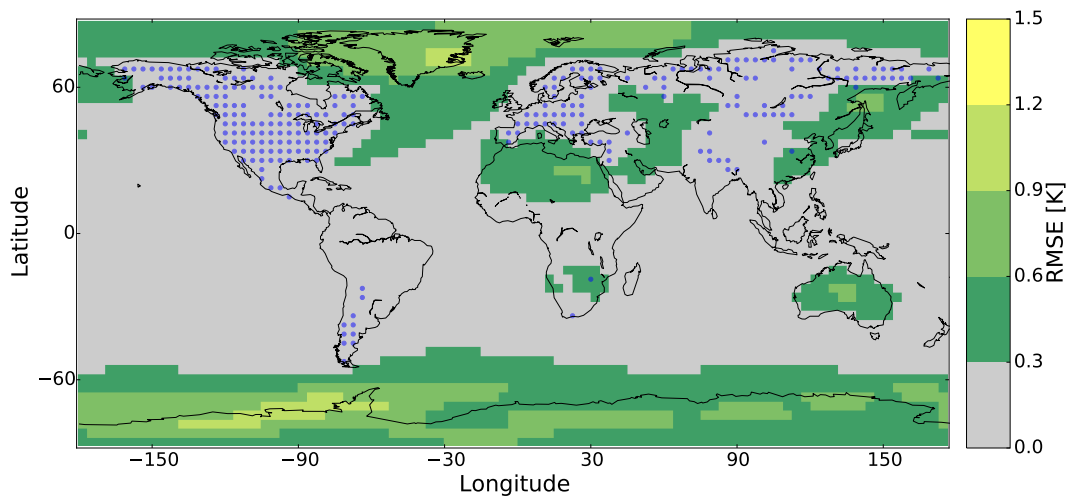
b) DA analysis for VSL-Prod with Leaky Bucket Model and nocycling
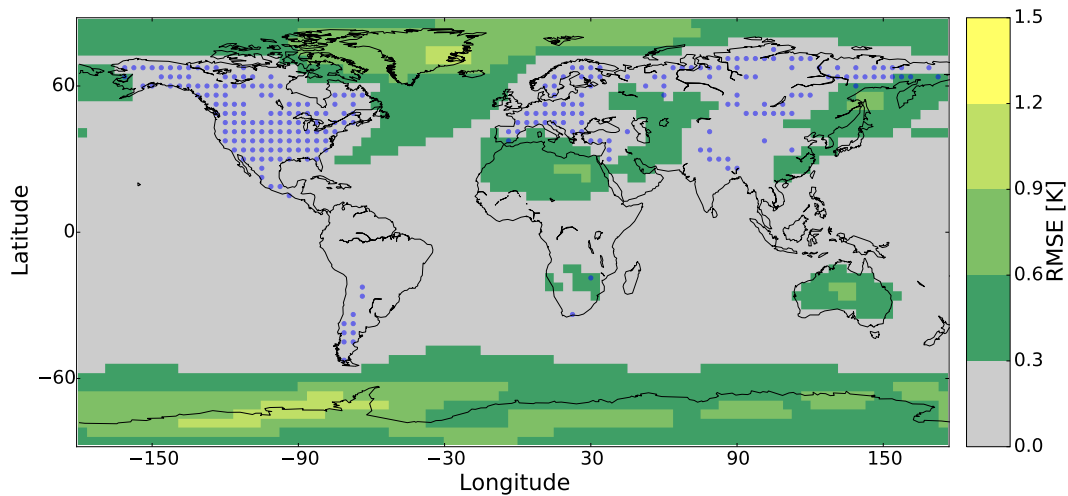
Figure 13. Time-averaged RMSEs of SLAB experiment for a) nocycling DA analysis using the VSL-Min with Leaky Bucket Model and b) the VSL-Prod with Leaky Bucket Model observation operator.
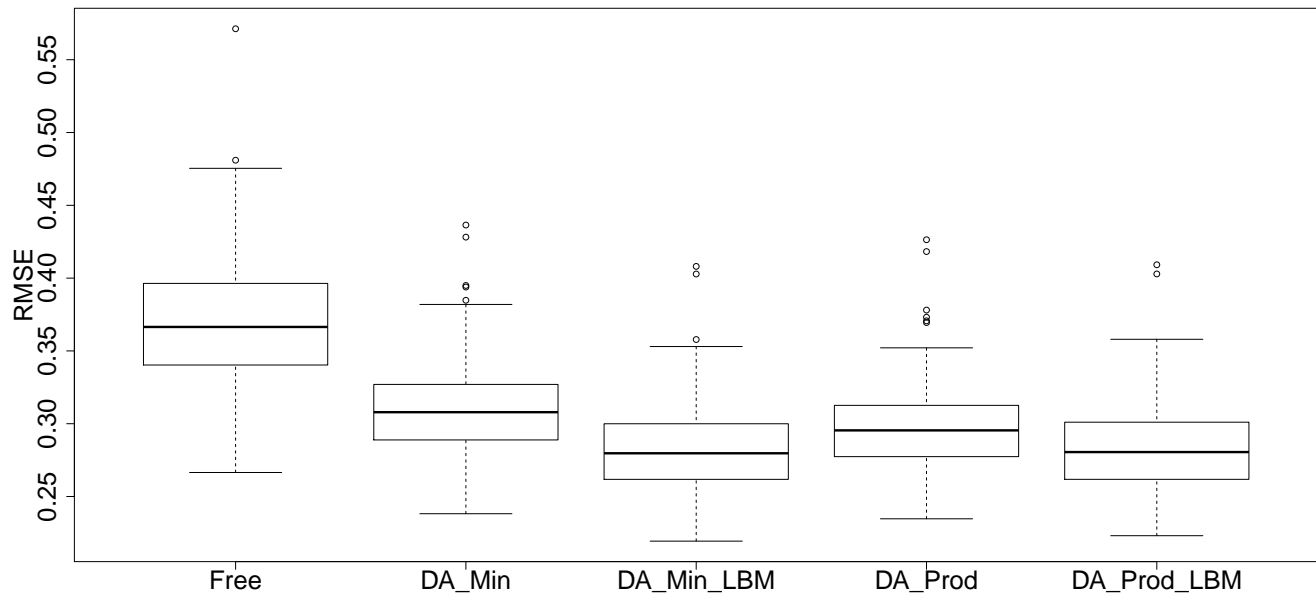
Figure 14. Histograms of global ensemble mean for analysis constrained by pseudo-TRW observations for Free run, DA run with VSL-Min, VSL-Prod using the climatological soil moisture and VSL-Min, VSL-Prod using the Leaky Bucket Model (LBM).